(12)

AD

TECHNICAL REPORT ARCCB-TR-87017

FATIGUE LIFE PREDICTION IN THICK-WALLED CYLINDERS WITH COMPLEX RESIDUAL STRESSES

S. L. PU

P. C. T. CHEN

JULY 1987

US ARMY ARMAMENT RESEARCH, DEVELOPMENT AND ENGINEERING CENTER
CLOSE COMBAT ARMAMENTS CENTER
BENÉT WEAPONS LABORATORY
WATERVLIET, N.Y. 12189-4050

DISCLAIMER

The findings in this report are not to be construed as an official Department of the Army position unless so designated by other authorized documents.

The use of trade name(s) and/or manufacturer(s) does not constitute an official indorsement or approval.

DESTRUCTION NOTICE

For classified documents, follow the procedures in DoD 5200.22-M, Industrial Security Manual, Section II-19 or DoD 5200.1-R, Information Security Program Regulation, Chapter IX.

For unclassified, limited documents, destroy by any method that will prevent disclosure of contents or reconstruction of the document.

For unclassified, unlimited documents, destroy when the report is no longer needed. Do not return it to the originator.

SECURITY CLASSIFICATION OF THIS PAGE (When Data Entered)

REPORT DOCUMENTATION PAGE

READ INSTRUCTIONS BEFORE COMPLETING FORM

1. REPORT NUMBER: ARCCB-TR-87017	2. GOVT ACCESSION NO.: A183599
3. RECIPIENT'S CATALOG NUMBER:	
4. TITLE (and Subtitle): FATIGUE LIFE PREDICTION IN THICK-WALLED CYLINDERS WITH COMPLEX RESIDUAL STRESSES	5. TYPE OF REPORT & PERIOD COVERED: Final
	6. PERFORMING ORG. REPORT NUMBER:
7. AUTHOR(s): S. L. Pu and P. C. T. Chen	8. CONTRACT OR GRANT NUMBER(s):
9. PERFORMING ORGANIZATION NAME AND ADDRESS: US Army ARDEC, Benet Weapons Laboratory, SMCAR-CCB-TL, Watervliet, NY 12189-4050	10. PROGRAM ELEMENT, PROJECT, TASK AREA & WORK UNIT NUMBERS: AMCMS No. 6111.02.H600.0, PRON No. 1A6DZ602NMSC
11. CONTROLLING OFFICE NAME AND ADDRESS: US Army ARDEC, Close Combat Armaments Center, Picatinny Arsenal, NJ 07806-5000	12. REPORT DATE: July 1987
	13. NUMBER OF PAGES: 20
14. MONITORING AGENCY NAME & ADDRESS (if different from Controlling Office):	15. SECURITY CLASS. (of this report): UNCLASSIFIED
	15a. DECLASSIFICATION/DOWNGRADING SCHEDULE:

16. DISTRIBUTION STATEMENT (of this Report)

Approved for public release; distribution unlimited.

17. DISTRIBUTION STATEMENT (of the abstract entered in Block 20, if different from Report)

18. SUPPLEMENTARY NOTES

Presented at ASTM National Symposium on Analytical and Experimental Methods for Residual Stress Effects in Fatigue, Phoenix, AZ, 20-21 October 1986. Published in Proceedings of the Symposium.

19. KEY WORDS (Continue on reverse side if necessary and identify by block number)

Fatigue Life
Radial Crack
Thick-Walled Cylinder
Stress-Intensity Range
Shape Factors
Negative K-Factor

20. ABSTRACT (Continue on reverse side if necessary and identify by block number)

The large variation in stress intensity factors corresponding to various material models for a single, radial, straight-fronted crack in a pressurized, partially autofrettaged cylinder leads to a drastic difference in the fatigue life predictions. None of the predicted lives agree with experimental results. Possible explanations of the discrepancy are given and corresponding correction factors are introduced. The predicted lives based on the corrected stress intensity ranges are reasonably close to a set of well-documented experimental results of Throop and Fujczak.

DD FORM 1 JAN 73 1473 EDITION OF 1 NOV 65 IS OBSOLETE

UNCLASSIFIED

SECURITY CLASSIFICATION OF THIS PAGE (When Data Entered)

TABLE OF CONTENTS

TABLES

LIST OF ILLUSTRATIONS

ACKNOWLEDGEMENT

We are grateful to J. H. Underwood for his valuable discussions, suggestions, and efforts to provide some old experimental data.

INTRODUCTION

Both finite element and modified mapping collocation methods have been used to obtain accurate stress intensity (K) solutions for pressurized autofrettaged thick cylinders with radial cracks (refs 1,2). Use of the weight function method has extended two-dimensional K solutions to more refined material models including reverse yielding caused by the Bauschinger effect (ref 3). Several papers have used stress intensity factors to estimate fatigue lives of cannon tubes (refs 4-6). The calculations underestimate the measured lives for pressurized cylinders, while they overestimate the experimental results for pressurized and autofrettaged cylinders (ref 5). The disagreement between measured and calculated lives diminishes in Reference 6 by introducing a fraction of the negative portion of K values as a part of the K range.

The shallow crack approximations for K solutions were used and a linear approximation for Bauschinger effect on residual hoop stress was assumed in References 5 and 6. The accurate two-dimensional K solutions affected by a significant Bauschinger effect using elastic-plastic analysis were used in Reference 7 to indicate the drastic effect of reverse yielding on the life prediction. Neither shape factors nor a fraction of negative K were considered in Reference 7.

In this report the life prediction formula similar to that used in Reference 7 is employed to check the calculated lives with experimental results of Throop (ref 8) and Throop and Fujczak (ref 9). The stress intensity factors for surface cracks of elliptical shape are approximated by the

---

References are listed at the end of this report.

two-dimensional stress intensity factors obtained in Reference 3 multiplied by respective shape factors for pressure and for residual stress given in Reference 5. The fraction of negative K included in K range varies from one at the notch boundary to zero at a crack depth far away from the notch. The variation of this fraction is assumed to be $1/r^2$ where r is the distance between the fatigue crack front and the notch front. Another modification is to use an initial crack depth much deeper than the notch depth. This is to avoid large cycles required in experiments to initiate a single continuous crack front along the notch boundary (it is considered likely (ref 5) that multiple, small, semi-elliptical cracks are initiated along the notch boundary prior to their link together to form a single crack). With these modifications the calculated lives agree reasonably well with experimental results for all three crack shapes: long curves, semi-elliptical, and semi-circular used in References 8 and 9.

FATIGUE LIFE PREDICTION

Integration of the Paris formula

$$\frac{da}{dN} = C(\Delta K)^m \tag{1}$$

for fatigue growth rate of a crack subjected to cyclic loading is usually used to determine the number of fatigue cycles required tc grow a crack from an initial depth a_i to a final depth a_f.

$$N = N_f - N_i = \int_{a_i}^{a_f} \frac{da}{C(\Delta K)^m} \tag{2}$$

where C and m are material constants and ΔK is the range of stress intensity defined by

$$\Delta K = K_{max} - K_{min} \tag{3}$$

K_{max} and K_{min} are maximum and minimum values of K in a loading cycle. Assume that a crack face is a geometric plane and there is no possibility of interpenetration under compression. This leads to a conclusion that K_{min} cannot be a negative value. In the case of repeated firing of cannon tubes

$$K_{min} = 0 \tag{4}$$

is used for both autofrettaged and nonautofrettaged tubes. If K_p and K_R denote mode I K values corresponding to an internal pressure and a residual hoop stress respectively, then

$$K_{max} = K_p \tag{5a}$$

for nonautofrettaged cylinders, and

$$K_{max} = K_p + K_R \tag{5b}$$

for autofrettaged cylinders. K_p and K_R are usually expressed in a dimensionless form denoted by f_{Kp} and f_{KR}, respectively,

$$f_{Kp} = \frac{K_p}{p\sqrt{\pi a}} \quad , \quad f_{KR} = \frac{K_R}{\sigma_o\sqrt{\pi a}} \tag{6}$$

where σ_o is the yield stress, p is the internal pressure applied to a tube, and p is related to σ_o by a load factor $f_L = \sigma_o/p$. By virtue of Eqs. (3), (4), and (5b)

$$\Delta K = \left(\frac{f_{Kp}}{f_L} + f_{KR}\right)\sigma_o\sqrt{\pi a} \tag{7}$$

For a small crack growth from a_j to a_{j+1}, f_{Kp} and f_{KR} are assumed to be constants which are taken as the mean values

$$\begin{aligned} \bar{f}_{Kp} &= \tfrac{1}{2}(f_{Kp}(a_j) + f_{Kp}(a_{j+1})) \\ \bar{f}_{KR} &= \tfrac{1}{2}(f_{KR}(a_j) + f_{KR}(a_{j+1})) \end{aligned} \tag{8}$$

The integration of Eq. (2) becomes

$$\frac{N}{C_o} = \frac{N_f - N_i}{C_o} = \sum_{j=1}^{n} 2^{-m}\left(\frac{\bar{f}_{KP}}{f_L} + \bar{f}_{KR}\right)^{-m}\left(\alpha_j^{1-m/2} - \alpha_{j+1}^{1-m/2}\right) \qquad (9)$$

where

$$C_o = \frac{2}{C(m-2)}\left(\frac{\sigma_o\sqrt{\pi}}{2}\right)^{-m}(t)^{1-m/2} \qquad (10)$$

with t denoting the wall thickness and $\alpha = a/t$. The fraction α is used since the crack depth is usually expressed as a fraction of wall thickness t.

Substituting from calculated values of f_{KP} and f_{KR} (ref 3) corresponding to various material models in Eqs. (8) and (9), we obtain the fatigue crack growth (α versus N/C_o) graph shown in Figure 1 for a single, two-dimensional straight-fronted through crack in a cylinder of diameter ratio two. In this figure, f is the Bauschinger effect factor. The dotted lines are for idealized material without Bauschinger effect (f = 1), while the dashed lines are for f = 0.38 (100 percent overstrain) and f = 0.44 (60 percent overstrain), respectively. The dashed lines with m' = 0 correspond to elastic-perfectly plastic behavior during reverse yielding. The dashed lines with m' = 0.3 indicate the difference in predicted cycles when strain-hardening is considered in reverse yielding. The graph shows the significant difference of autofrettage effect of various material models on fatigue cycles. Such a drastic difference is not supported by experimental results. Corrective parameters must be introduced to correlate the calculated fatigue cycles with observed ones in laboratory tests.

SHAPE FACTORS

The ratio of stress intensity factor for a surface crack to that of a two-dimensional through crack is called the shape factor. The stress intensity factor varies along the crack front of a surface crack. It changes with

crack shape and under different loadings. If the variation of stress intensity along the crack front is important, the three-dimensional K solutions for the surface crack should be obtained. If an estimate of K at a point, say the deepest point of the surface crack, is needed, then a reasonable estimate of shape factor is useful. An extensive study of shape factors has been published by Newman and Raju (ref 10) for semi-elliptical cracks in a flat plate under tension or bending. There is no comparable study for such a crack in a thick cylinder. Parker et al (ref 5) obtained estimates of shape factors for semi-elliptical cracks of various aspect ratios in a pressurized and auto-frettaged cylinder from judicious use of results reported in Reference 10. More accurate three-dimensional K solutions should be obtained to check these estimates. Before more accurate and reliable shape factors become available, values close to those given by (a) and (c) of Figure 7 in Reference 5 are used for f_{Sp} and f_{SR}, respectively, in this study. Multiplying f_{Kp} and f_{KR} with their shape factors, Eq. (7) becomes

$$\Delta K = \left(\frac{f_{Sp}f_{Kp}}{f_L} + f_{SR}f_{KR}\right)\sigma_o\sqrt{\pi a} \tag{11}$$

The following mean values are used in Eq. (11) for a small crack growth from a_j to a_{j+1}.

$$\begin{aligned}\overline{f_{Sp}f_{Kp}} &= \tfrac{1}{2}[f_{Sp}(a_j)f_{Kp}(a_j) + f_{Sp}(a_{j+1})f_{Kp}(a_{j+1})] \\ \overline{f_{SR}f_{KR}} &= \tfrac{1}{2}[f_{SR}(a_j)f_{KR}(a_j) + f_{SR}(a_{j+1})f_{KR}(a_{j+1})]\end{aligned} \tag{12}$$

NEGATIVE K FACTOR F_N

For a fatigue crack which is considered as a geometrical plane with no thickness, $K_{min} = 0$ is used in Eq. (3) to obtain K range. For a notch with finite thickness, the upper and lower planes of the notch may have normal

displacement in both directions. The argument used to limit $K_{min} = 0$ is not valid at the notch front. In fact, the full negative K should be used for a crack starting at the notch. At some depth, the notch effect may become negligibly small, and $K_{min} = 0$ may again be used in Eq. (3) for ΔK. Kendall has argued that a portion of the negative K must be included in calculating K range (ref 6). He introduced a constant fraction which is multiplied by the negative K (K_R) coresponding to compressive residual stress due to autofrettage to give the K_{min} in ΔK. From our hypothesis, the fraction varies with the depth of the fatigue crack. As a first approximation, the fraction f_N is taken as $(1 + r/r_n)^{-a}$ where r_n is the depth of the notch and r is the depth of the crack measured from the notch front. At the notch front $r = 0$ and $f_N = 1$, the full negative K is taken as K_{min}. When $r = r_n$ the fatigue crack grows to a depth equal to the notch depth; this approximation gives $f_N = \frac{1}{4}$. It is also assumed that $f_N = 0$ when $r > 2r_n$. A linear variation of f_N was another approximation examined which underestimated the measured fatigue lives.

Incorporating f_N, Eq. (11) becomes

$$\Delta K = [f_{Sp} \frac{f_{Kp}}{f_L} + (1-f_N) f_{SR} f_{KR}] \sigma_o \sqrt{\pi a} \tag{13}$$

Equation (9) can be expressed explicitly

$$\frac{N}{C_o} = \sum_{j=1}^{n} [\frac{\tilde{f}_{Kp}(\alpha_j) + \tilde{f}_{Kp}(\alpha_{j+1})}{f_L} + \tilde{f}_{KR}(\alpha_j) + \tilde{f}_{KR}(\alpha_{j+1})]^{-m} (\alpha_j^{1-m/2} - \alpha_{j+1}^{1-m/2}) \tag{14}$$

where abbreviations $\tilde{f}_{Kp}$, $\tilde{f}_{KR}$ are

$$\begin{aligned} \tilde{f}_{Kp}(\alpha_j) &= f_{Sp}(\alpha_j) f_{Kp}(\alpha_j) \\ \tilde{f}_{KR}(\alpha_j) &= [1 - f_N(\alpha_j)] f_{SR}(\alpha_j) f_{KR}(\alpha_j) \end{aligned} \tag{15}$$

LABORATORY SPECIMENS AND MEASURED LIVES

Throop (ref 8) and Throop and Fujczak (ref 9) obtained a series of experimental results which relate fatigue crack lives with crack shape and extent of autofrettage for thick-wall cylinders. The cylinders were 0.76 m (30 inches) in length, 180 mm (7.1 inches) bore diameter, 360 mm (14.25 inches) outside diameter and were fatigue cracked from longitudinal internal notches. Three initial notch geometries were used; semi-circular, 100 mm (4-inch) and 500 mm (20-inch) long notches produced by electrical discharging machining. They were 6.4 mm (¼-inch) deep by 0.76 mm (0.03-inch) wide, the semi-circular notch being 13 mm (½-inch) diameter half-penny shape. Fatigue cracks grown from the initial notches were monitored periodically for depth and shape with ultrasonics as the cylinder was repeatedly pressurized to 330 MPa (48 Ksi). The cylinder material was ASTM A723 forged steel, with yield strength of 1175 MPa, -40°C Charpy impact energy of 34 J, reduction in area of 50 percent. A schematic diagram of a typical cylinder with a simple initial notch and the growth of a 500 mm (20-inch) long notch from 6.4 mm (¼-inch) initial depth by repeated pressurization is shown in Figure 2. The measured crack depth versus corresponding number of fatigue loadings is shown in Figure 3 for a single-notched cylinder with 0, 30, and 60 percent overstrains for three-notch geometries.

Since the fatigue crack is not likely to start from the notch immediately, an adjustment of experimental results is made by subtracting the number of cycles required to grow from initial notch depth to an initial crack depth (a_i) from the number of cycles to grow from initial notch depth to a final crack depth (a_f). The initial crack depth, which should be reasonably

larger than the initial notch depth (6.4 mm in this experimental study), is arbitrarily taken as $a_i = 0.1t = 9$ mm. The original experimental data are available only in graphs. To improve the accuracy of readings from graphs, the graphs were first enlarged and the average was used from values obtained from different graphs published in different papers (refs 4,5,9) for the same set of experimental data. The adjusted experimental results are shown by dots in Figures 4, 5, 6, and 7.

PREDICTED LIVES FOR THE EXPERIMENTS

The material constants for the steel used in the experiments are $m = 3$ and $C = 6.52 \times 10^{-12}$ for crack growth in meters per cycle and ΔK in MPa$\sqrt{\text{meter}}$ (or $C = 3.4 \times 10^{-10}$ for crack growth in inches per cycle and ΔK in Ksi$\sqrt{\text{inch}}$). Using $f_L = 3.55$ and values of f_{Sp} and f_{SR} in Table I, and assuming $f_N = (1 + r/r_n)^{-2}$ for $0 < r < 2r_n$ and $f_N = 0$ for $r > 2r_n$, Eqs. (14) and (15) can be evaluated with known discrete values of f_{Kp} and f_{KR}. Values of f_{Sp} and f_{SR}, given in Table I, are obtained from Reference 5 for different crack geometries. Discrete values of f_{Kp} and f_{KR} can be computed by the method described in Reference 3. The calculated lives and measured lives are plotted in Figures 4, 5, and 6 for three crack geometries, respectively. For nonautofrettaged cylinders (zero percent overstrain), there is only one set of calculated results, shown in a solid line, for each crack configuration. For 60 percent overstrain, solid lines are for idealized material without considering the Bauschinger effect, while two dashed lines in each figure are predicted lives with some reverse yielding. The two dashed lines differ in m' values, $m' = 0$ or 0.3, where m'E is the slope of strain-hardening during reverse yielding.

When m' = 0, the material behaves like elastic-perfectly plastic in reverse yielding. The magnitude of the compressive, residual stress in the tangential direction near the bore is smaller than that in a strain-hardening material (ref 3). The strain-hardening reduces the adverse effect of reverse yielding due to the Bauschinger effect, Figure 1. Figures 4 through 6 show an overall effect of all factors. Figure 7 shows the effect of each factor on the semi-elliptical surface crack in a pressurized cylinder with 60 percent overstrain. The dotted curve, curve 1, gives the calculated lives for an idealized material with no Bauschinger effect. No correction factors are used. The stress intensity range is based on two-dimensional stress intensity factors and $K_{min} = 0$. If the change in residual hoop stress due to the Bauschinger effect (Bauschinger effect factor f = 0.44) is considered, the calculated lives are shown as a dashed curve, curve 2, where m' = 0.3 is used. The large difference between curves 1 and 2 shows the significant effect of reverse yielding on fatigue lives. If shape factors f_{Sp} and f_{SR} are considered in addition to the Bauschinger effect, the predicted lives will be changed from curve 2 to curve 3. The shape factors are to increase the fatigue lives. Finally, if the correction factor f_N is also taken into consideration, the predicted lives are shown as the solid line, curve 4, which is close to the experimental results shown by dots in Figure 7. Similar graphs, obtained for the long curved crack and the semi-circular crack, are omitted since they indicate similar effects of each correction factor.

TABLE I. VALUES OF f_{Sp} AND f_{SR} FOR DIFFERENT CRACK GEOMETRIES

$\alpha = a/t$	20-Inch Long Notch		4-Inch Long Notch		Semi-Circular Notch	
	f_{Sp}	f_{SR}	f_{Sp}	f_{SR}	f_{Sp}	f_{SR}
0.1	0.95	0.95	0.72	0.69	0.57	0.58
0.2	0.90	0.90	0.64	0.60	0.53	0.52
0.3	0.85	0.85	0.61	0.55	0.51	0.42
0.4	0.85	0.80	0.57	0.47	0.48	0.34
0.5	0.85	0.75	0.56	0.38	0.44	0.24

CONCLUSIONS

The fatigue life of a thick-walled cylinder can be predicted reasonably well by integration of the Paris formula for growth rate of a fatigue crack under cyclic loading, if a modified stress intensity range is used. The stress intensity range is obtained by multiplying two-dimensional stress intensity factors by proper shape factors and some negative K factors. More systematic and controlled experiments are required to check the idea proposed in this report. Three-dimensional K solutions for semi-elliptical surface cracks in thick cylinders with various residual stresses are needed to estimate the proper shape factors. Special experiments should be performed to verify the concept of negative K factors and to determine the variation of f_N in terms of crack depth.

REFERENCES

1. Parker, A. P., "Stress Intensity and Fatigue Crack Growth in Multiply Cracked, Pressurized, Partially Autofrettaged Thick Cylinders," Fatigue of Engineering Materials and Structures, Vol. 4, No. 2, 1982.

2. Pu, S. L. and Hussain, M. A., "Stress-Intensity Factors For Radial Cracks in a Partially Autofrettaged Thick-Wall Cylinder," Fracture Mechanics: Fourteenth Symposium - Volume I: Theory and Analysis, ASTM STP 791, 1983, pp. I-194-I-215.

3. Pu, S. L. and Chen, P. C. T., "The Bauschinger Effect on Stress Intensity Factors For a Radially Cracked Gun Tube," Transactions of the Third Army Conference on Applied Mathematics and Computing, Georgia Institute of Technology, ARO Report 86-1, 1986, pp. 275-294.

4. Underwood, J. H. and Throop, J. F., "Surface Crack K-Estimates and Fatigue Life Calculations in Cannon Tubes," Part-Through Crack Fatigue Life Prediction, ASTM STP 687, 1979, pp. 195-210.

5. Parker, A. P., Underwood, J. H., Throop, J. F., and Andrasic, C. P., "Stress Intensity and Fatigue Crack Growth in a Pressurized, Autofrettaged Thick Cylinder," Fracture Mechanics: Fourteenth Symposium - Volume I: Theory and Analysis, ASTM STP 791, 1983, pp. I-216-I-237.

6. Kendall, D. P., "A Simple Fracture Mechanics Based Method for Fatigue Life Prediction in Thick-Walled Cylinders," Technical Report ARLCB-TR-84023, Benet Weapons Laboratory, Watervliet, NY, July 1984.

7. Pu, S. L. and Sha, G. T., "The Bauschinger Effect of Reverse Yield Stress Reduction on Radial Crack Growth of a Cylindrical Pressure Vessel," Engineering Fracture Mechanics, Vol. 26, No. 4, 1987, pp. 519-531.

8. Throop, J. F., "Fatigue Crack Growth in Thick-Walled Cylinders," Proceedings of National Conference on Fluid Power, Vol. XXVI, 1972, pp. 115-131.

9. Throop, J. F. and Fujczak, R. R., "Strain Behavior of Pressurized Cracked Thick-Walled Cylinders," Experimental Mechanics, Vol. 22, 1982, pp. 277-286.

10. Newman, J. C. and Raju, I. S., "Analyses of Surface Cracks in Finite Plates Under Tension or Bending Loads," NASA TP 1578, National Aeronautics and Space Administration, Washington D.C., 1979.

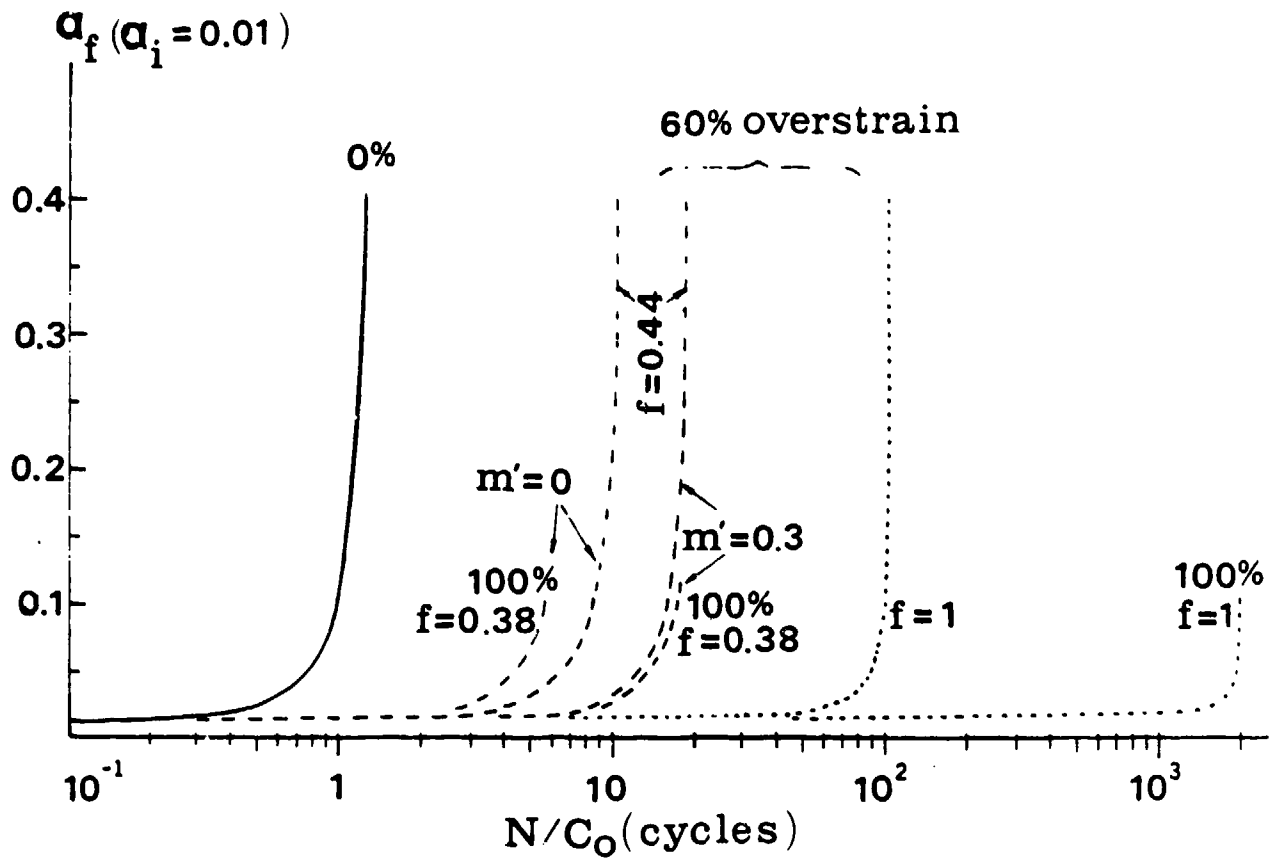

Figure 1. Effect of reverse yielding on fatigue crack growth shown in a (a versus N/C_o) plot for a 2.0 diameter ratio cylinder with a single, straight-fronted through crack.

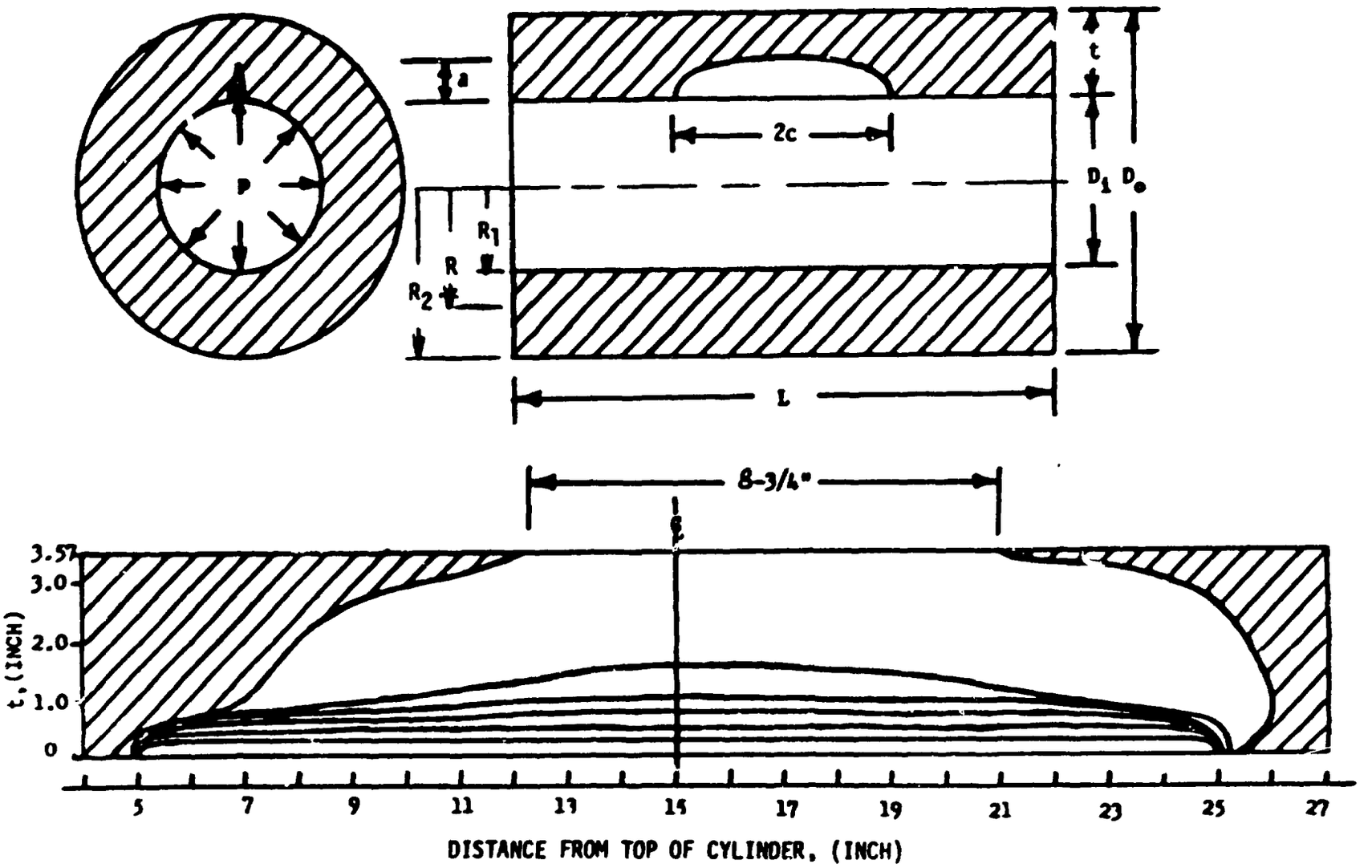

Figure 2. A schematic diagram of a cylinder specimen with initial 20-inch long notch and the growth of the notch by repeated pressurization (ref 9).

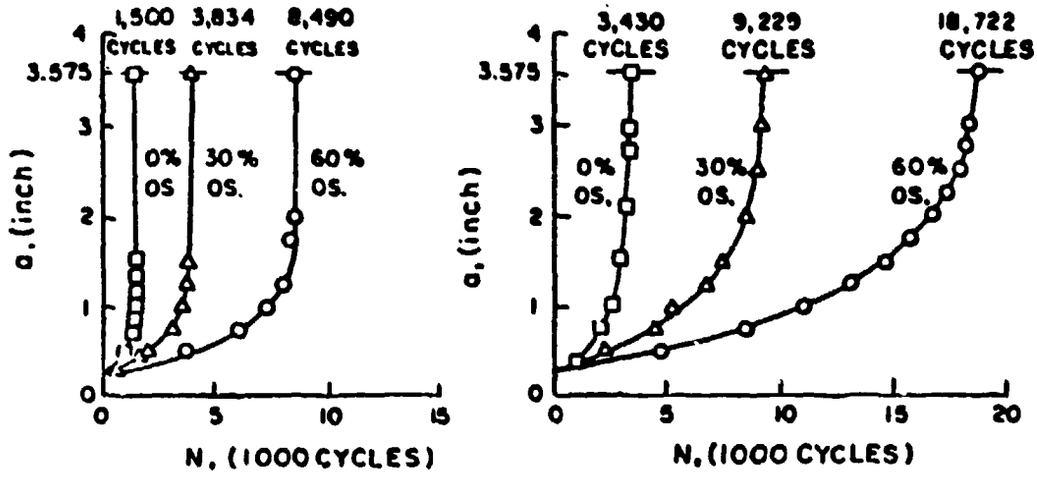

(a) LONG CURVED CRACK

(b) SEMI-ELLIPTICAL CRACK

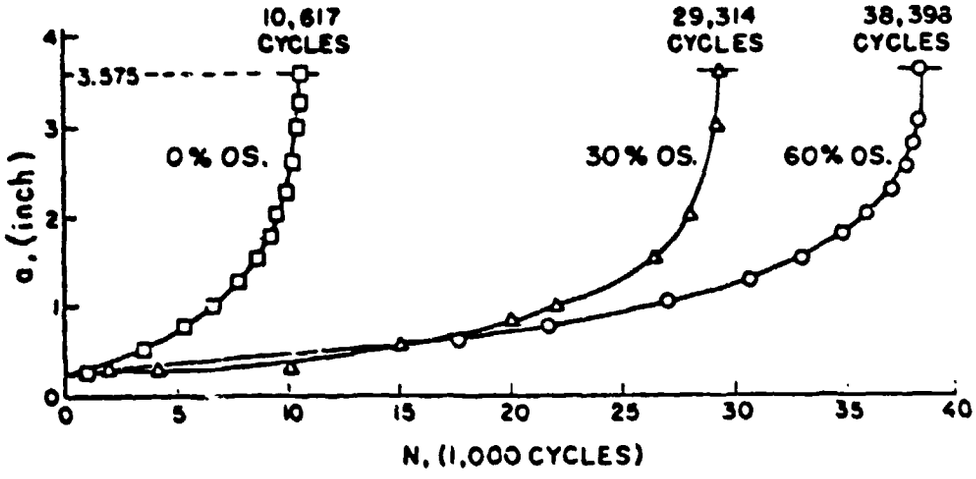

(c) SEMI-CIRCULAR CRACK

Figure 3. Crack depth plotted versus number of fatigue loadings - experimental results (ref 9).

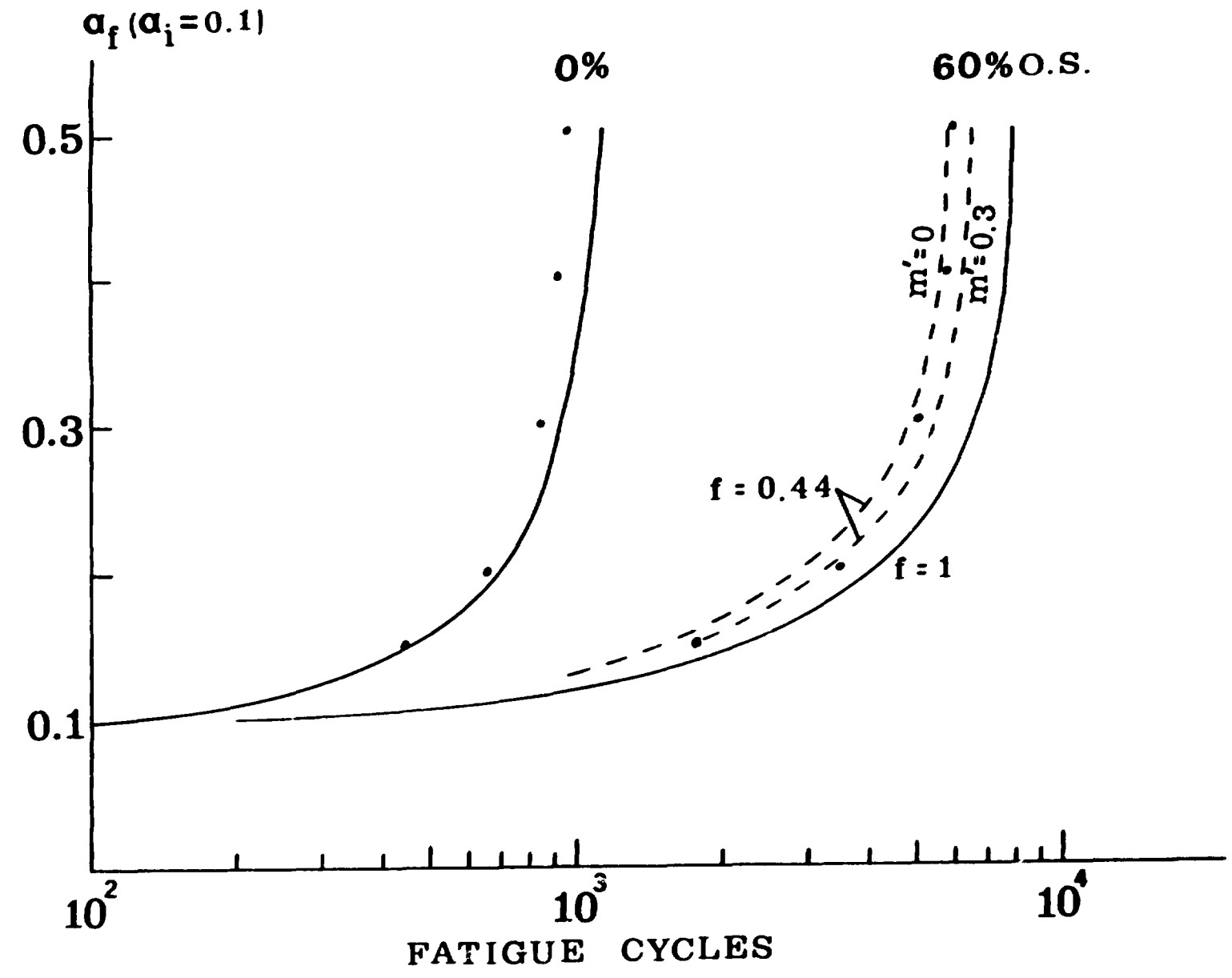

Figure 4. Crack depth versus fatigue cycles for long curved cracks. Dots: experimental results, lines: calculated results.

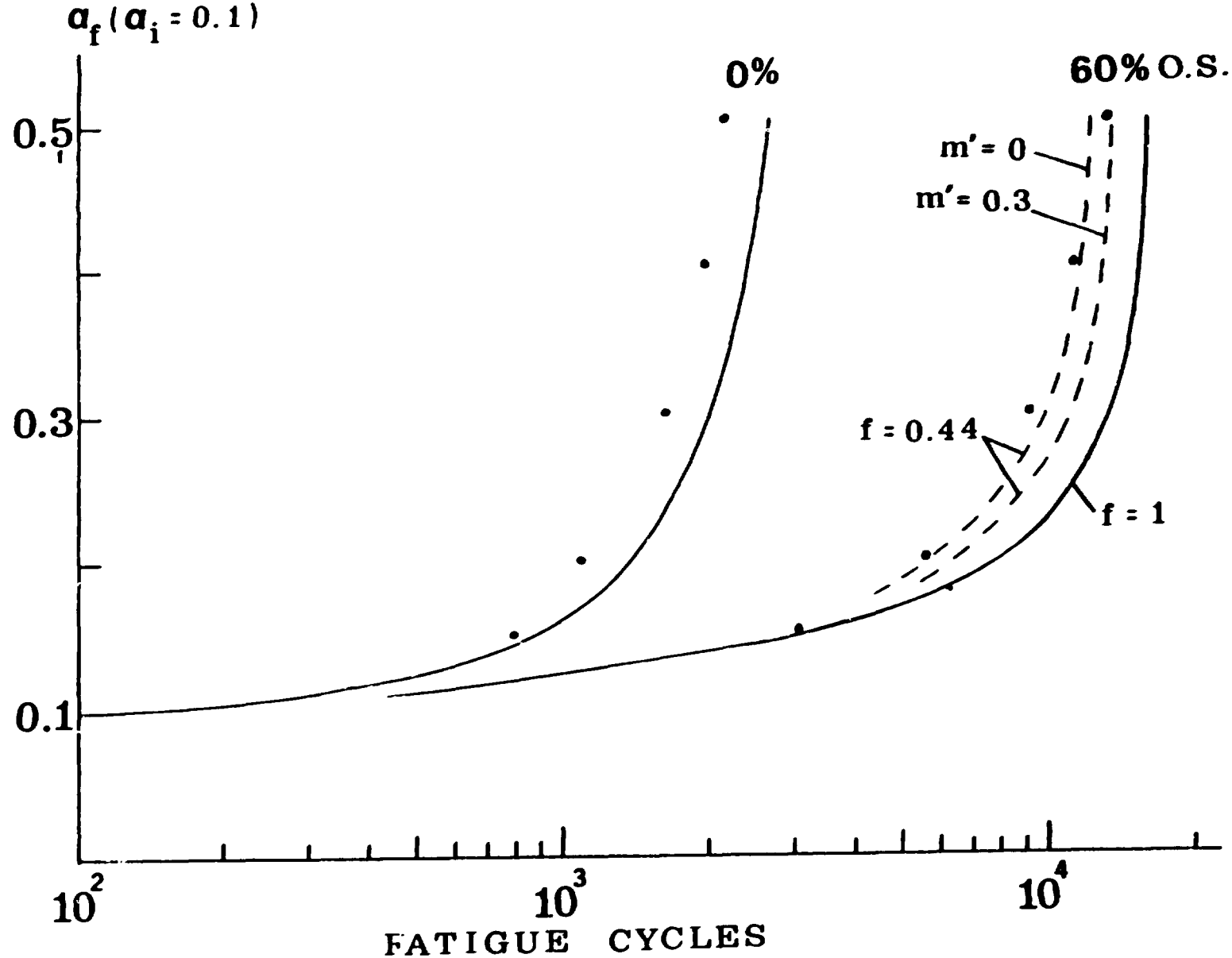

Figure 5. Crack depth versus fatigue cycles for semi-elliptical cracks. Dots: experimental results, lines: calculated results.

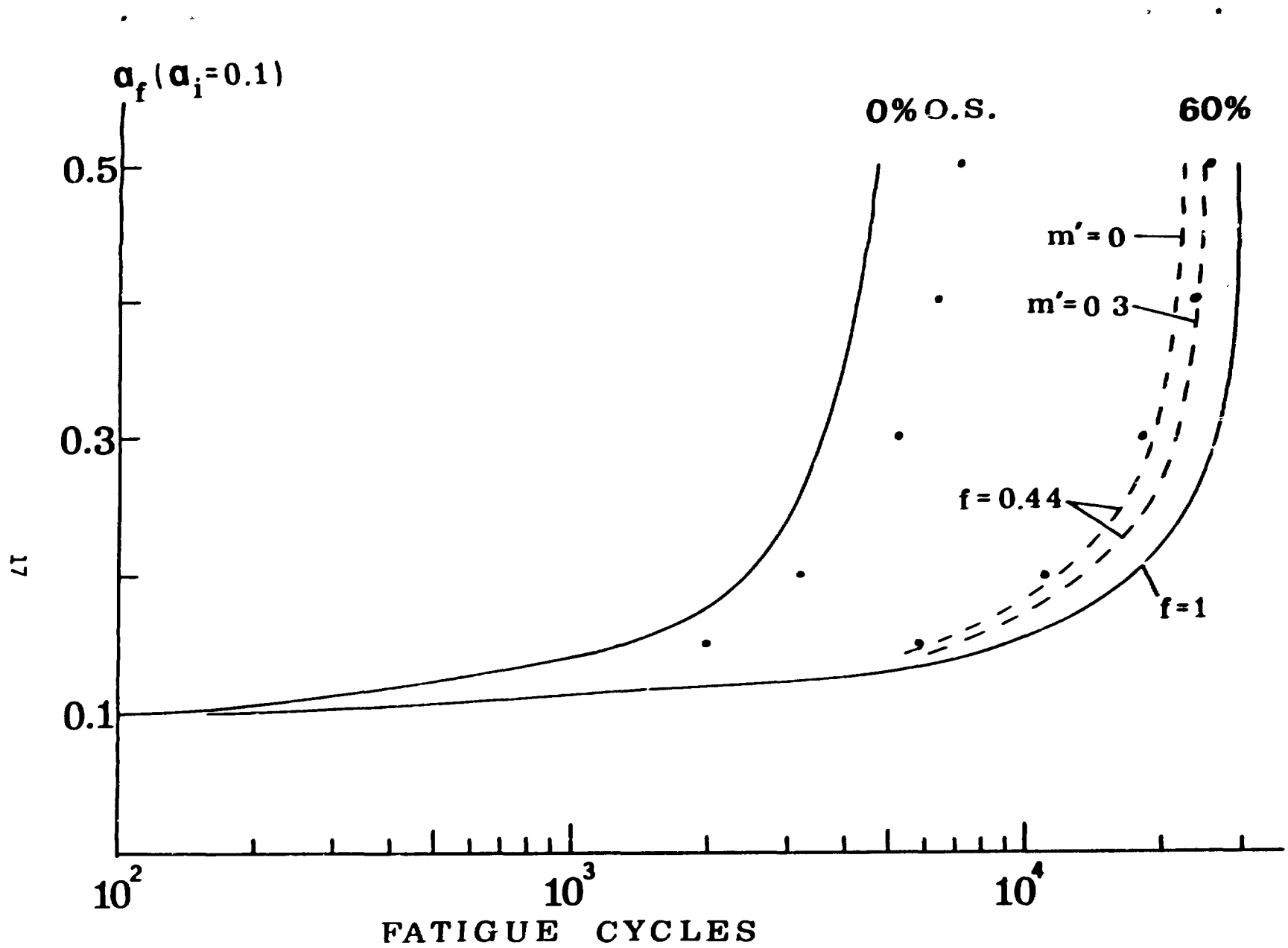

Figure 6. Crack depth versus fatigue cycles for semi-circular cracks. Dots: experimental results, lines: calculated results.

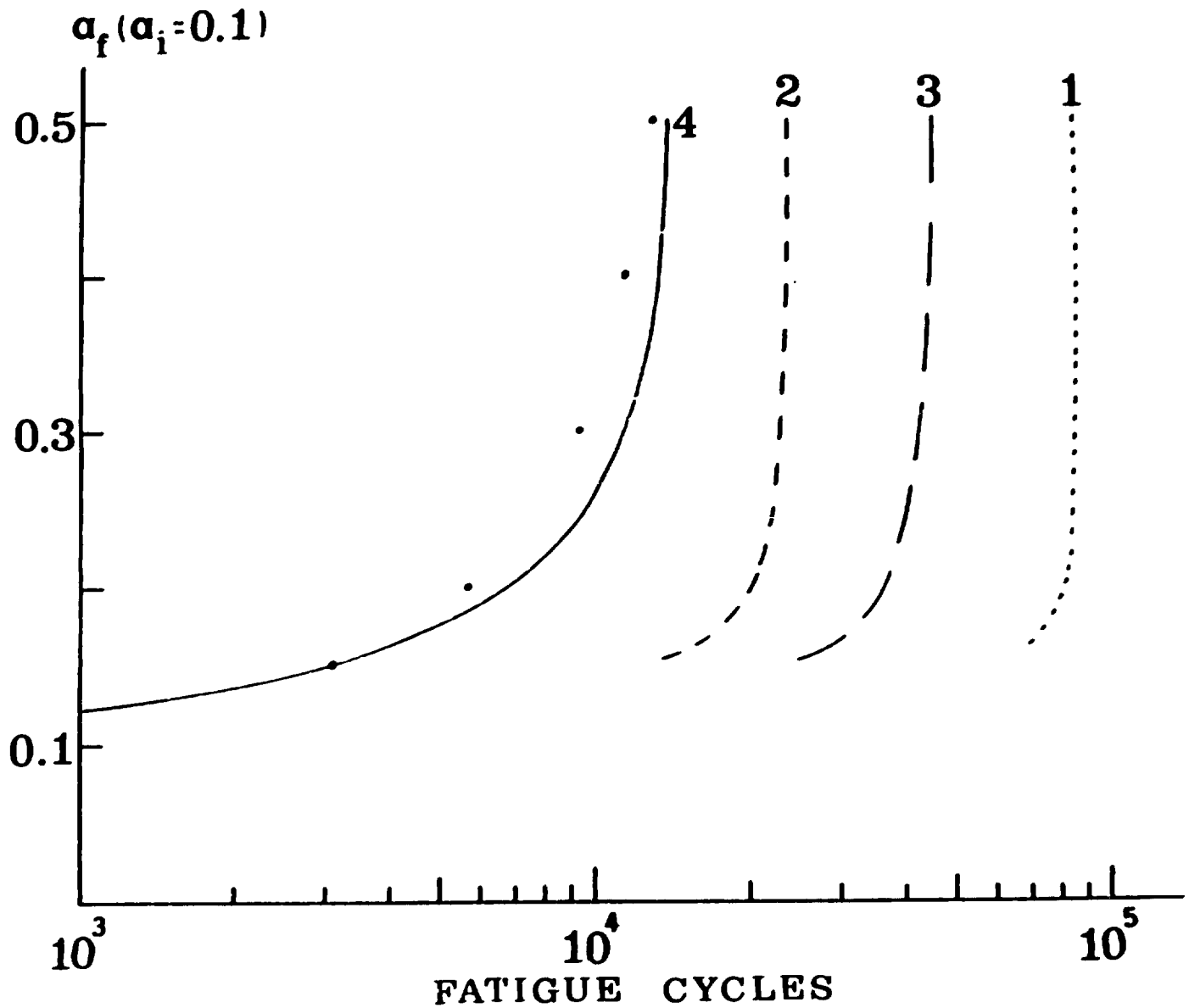

Figure 7. Effect on fatigue cycles of various correction factors for a semi-elliptical surface crack in a pressurized, 60 percent autofrettaged cylinder.

TECHNICAL REPORT INTERNAL DISTRIBUTION LIST

	NO. OF COPIES
CHIEF, DEVELOPMENT ENGINEERING BRANCH	
ATTN: SMCAR-CCB-D	1
-DA	1
-DC	1
-DM	1
-DP	1
-DR	1
-DS (SYSTEMS)	1
CHIEF, ENGINEERING SUPPORT BRANCH	
ATTN: SMCAR-CCB-S	1
-SE	1
CHIEF, RESEARCH BRANCH	
ATTN: SMCAR-CCB-R	2
-R (ELLEN FOGARTY)	1
-RA	1
-RM	1
-RP	1
-RT	1
TECHNICAL LIBRARY	
ATTN: SMCAR-CCB-TL	5
TECHNICAL PUBLICATIONS & EDITING UNIT	
ATTN: SMCAR-CCB-TL	2
DIRECTOR, OPERATIONS DIRECTORATE	
ATTN: SMCWV-OD	1
DIRECTOR, PROCUREMENT DIRECTORATE	
ATTN: SMCWV-PP	1
DIRECTOR, PRODUCT ASSURANCE DIRECTORATE	
ATTN: SMCWV-QA	1

NOTE: PLEASE NOTIFY DIRECTOR, BENET WEAPONS LABORATORY, ATTN: SMCAR-CCB-TL, OF ANY ADDRESS CHANGES.

TECHNICAL REPORT EXTERNAL DISTRIBUTION LIST

	NO. OF COPIES
ASST SEC OF THE ARMY RESEARCH AND DEVELOPMENT ATTN: DEPT FOR SCI AND TECH THE PENTAGON WASHINGTON, D.C. 20310-0103	1
ADMINISTRATOR DEFENSE TECHNICAL INFO CENTER ATTN: DTIC-FDAC CAMERON STATION ALEXANDRIA, VA 22304-6145	12
COMMANDER US ARMY ARDEC ATTN: SMCAR-AEE	1
SMCAR-AES, BLDG. 321	1
SMCAR-AET-O, BLDG. 351N	1
SMCAR-CC	1
SMCAR-CCP-A	1
SMCAR-FSA	1
SMCAR-FSM-E	1
SMCAR-FSS-D, BLDG. 94	1
SMCAR-MSI (STINFO) PICATINNY ARSENAL, NJ 07806-5000	2
DIRECTOR US ARMY BALLISTIC RESEARCH LABORATORY ATTN: SLCBR-DD-T, BLDG. 305 ABERDEEN PROVING GROUND, MD 21005-5066	1
DIRECTOR US ARMY MATERIEL SYSTEMS ANALYSIS ACTV ATTN: AMXSY-MP ABERDEEN PROVING GROUND, MD 21005-5071	1
COMMANDER HQ, AMCCOM ATTN: AMSMC-IMP-L ROCK ISLAND, IL 61299-6000	1
COMMANDER ROCK ISLAND ARSENAL ATTN: SMCRI-ENM ROCK ISLAND, IL 61299-5000	1
DIRECTOR US ARMY INDUSTRIAL BASE ENGR ACTV ATTN: AMXIB-P ROCK ISLAND, IL 61299-7260	1
COMMANDER US ARMY TANK-AUTMV R&D COMMAND ATTN: AMSTA-DDL (TECH LIB) WARREN, MI 48397-5000	1
COMMANDER US MILITARY ACADEMY ATTN: DEPARTMENT OF MECHANICS WEST POINT, NY 10996-1792	1
US ARMY MISSILE COMMAND REDSTONE SCIENTIFIC INFO CTR ATTN: DOCUMENTS SECT, BLDG. 4484 REDSTONE ARSENAL, AL 35898-5241	2
COMMANDER US ARMY FGN SCIENCE AND TECH CTR ATTN: DRXST-SD 220 7TH STREET, N.E. CHARLOTTESVILLE, VA 22901	1
COMMANDER US ARMY LABCOM MATERIALS TECHNOLOGY LAB ATTN: SLCMT-IML (TECH LIB) WATERTOWN, MA 02172-0001	2

NOTE: PLEASE NOTIFY COMMANDER, ARMAMENT RESEARCH, DEVELOPMENT, AND ENGINEERING CENTER, US ARMY AMCCOM, ATTN: BENET WEAPONS LABORATORY, SMCAR-CCB-TL, WATERVLIET, NY 12189-4050, OF ANY ADDRESS CHANGES.

TECHNICAL REPORT EXTERNAL DISTRIBUTION LIST (CONT'D)

	NO. OF COPIES
COMMANDER US ARMY LABCOM, ISA ATTN: SLCIS-IM-TL 2800 POWDER MILL ROAD ADELPHI, MD 20783-1145	1
COMMANDER US ARMY RESEARCH OFFICE ATTN: CHIEF, IPO P.O. BOX 12211 RESEARCH TRIANGLE PARK, NC 27709-2211	1
DIRECTOR US NAVAL RESEARCH LAB ATTN: DIR, MECH DIV CODE 26-27 (DOC LIB) WASHINGTON, D.C. 20375	1 1
COMMANDER AIR FORCE ARMAMENT LABORATORY ATTN: AFATL/MN EGLIN AFB, FL 32543-5434	1
COMMANDER AIR FORCE ARMAMENT LABORATORY ATTN: AFATL/MNG EGLIN AFB, FL 32542-5000	1
METALS AND CERAMICS INFO CTR BATTELLE COLUMBUS DIVISION 505 KING AVENUE COLUMBUS, OH 43201-2693	1

NOTE: PLEASE NOTIFY COMMANDER, ARMAMENT RESEARCH, DEVELOPMENT, AND ENGINEERING CENTER, US ARMY AMCCOM, ATTN: BENET WEAPONS LABORATORY, SMCAR-CCB-TL, WATERVLIET, NY 12189-4050, OF ANY ADDRESS CHANGES.